

DESIGN OF A FAST LONG RANGE ACTUATOR – FLORA II

Erik M. Zdanowicz, Jeffrey W. Eischen, and Thomas A. Dow
Precision Engineering Center
North Carolina State University
Raleigh, North Carolina, USA

INTRODUCTION

The objective of this NSF sponsored research is to develop machinery to fabricate Non-Rotationally Symmetric (NRS) optical surfaces. NRS surfaces have typically been machined using very slow spindle speeds or actuators with a limited range of several hundred μm . This means only limited surface features can be machine or the process takes a long time. A Fast Long Range Actuator (FLORA) has been constructed [1] with a goal of machining NRS surfaces with a range of motion of $\pm 2\text{ mm}$ at 20 Hz. For the surface to have the same quality as conventional diamond turning machines the surface must have a form error of less than 150 nm peak-to-valley and a surface finish of 5 nm RMS.

The FLORA system consists of a triangular aluminum honeycomb piston supported by orifice type air bearings and driven by a linear motor. While machining with FLORA was successful, the system dimensions are large when compared with the range of motion and the size of the tool and the piston weighed 650 grams. In addition, the air bearing on the FLORA has 200 nm of vertical vibration which has an impact on the surface finish possible.

A new design, FLORA II, has been created to address the limitations of its predecessor. The FLORA II package is smaller and lighter than FLORA while maintaining bearing stiffness and improving system dynamics. This was accomplished through structural analysis supplemented with experimental testing. The design described in this paper will show how the FLORA II can produce high quality NRS optical surfaces from a small, lightweight system.

AIR BEARINGS

One of the main features in the FLORA design is the air bearing. This bearing eliminates friction, supports the tool with little or no deflection and moves piston in a straight line. The original FLORA design had orifice-type air bearings that consist of a number of small orifices along the

bearing surface to create the pressurized air film that supports the piston. It is believed that these bearings are responsible for the 200 nm vertical vibration of FLORA [1]. For this reason, FLORA II was designed with porous-carbon air bearings. Porous air bearings are constructed with an aluminum backing that acts as a manifold to distribute air through a porous carbon material. This porous carbon material has millions of small holes for air distribution and creates a nearly uniform pressure distribution over the surface of the bearing. Orifice type bearings have more pressure variation over the face of the bearing.

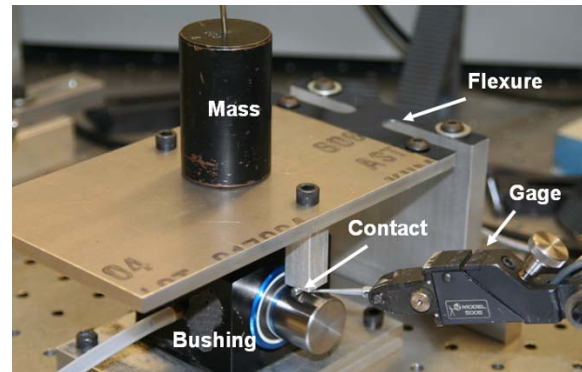


FIGURE 1. Radial stiffness test.

Finite Element Analysis (FEA) software is a powerful design tool that if used properly, can provide important information such as deformation of a complex body under load. The software ANSYS has an elastic foundation type of support which attaches a bed-of-springs from a moving part to a fixed support. This bed-of-springs foundation can be used to approximate the stiffness of the air bearing provided by the pressurized air. The company that makes the porous bearings, New Way [2], publishes an overall stiffness for their bearings at a certain pressure. To use the bed-of-springs approach, ANSYS requires specification of stiffness per unit area. Therefore, equivalent foundation stiffness had to be derived from the stiffness provided by New Way for use in the ANSYS

model. To verify the model, a 25 mm diameter air bushing shown in Figure 1 was purchased. The air bushing consists of a hollow aluminum tube with the carbon bearing material on the inside. A circular shaft rides in the bearing with a radial film thickness of about 5 μm . The aluminum tube is supported by 4 O-rings and an epoxy resin is injected between the tube and housing to rigidly support the bearing.

Air Bearing Experiment

Static and dynamic experiments were run on the test bushing in order to verify theoretical derivations. The tests consisted of the 25 mm bushing, a 110 mm long stainless steel shaft, a flexure loading device, and a mounting block. Epoxy adhesive applied between the bushing and support block eliminated any effect the O-rings had on the bearing stiffness.

Static Air Bearing Measurements

New Way provides two stiffness values for each bushing: radial and pitch. Radial stiffness is the load required to produce a unit value of radial translation of the shaft. Pitch is the moment required to produce a unit rotation of the shaft in the bushing. Figure 2 shows the radial and pitch directions.

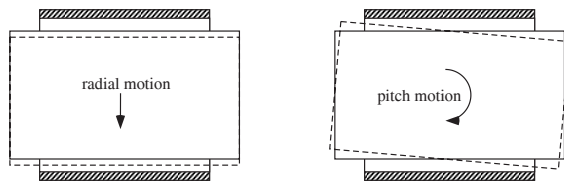


FIGURE 2. Pitch motion is shown on the left while radial motion is shown on the right.

The first static test was to verify the radial stiffness of the bushing. This is the stiffness of vertical translation of the shaft inside the bushing. The experiment was run as shown in Figure 1. The known mass was placed on the center of a load plate that was hinged to a vertical support by a thin flexure. The flexure had cut outs from the sides to allow the plate to twist so the contacts would apply equal loads to each end of the shaft. The contacts had small cylinders glued to the ends so as to apply a point contact. A lever-type gage head was used to measure the displacement under the contact. Three different known masses were placed on the load plate 10 times each and the displacements were recorded. From these experiments it was found that the radial stiffness

was 25.8 $\text{N}/\mu\text{m}$. This value is close to the 27.9 $\text{N}/\mu\text{m}$ predicted using the value (34 $\text{N}/\mu\text{m}$) [2] published by New Way reduced due to the bending stiffness of the steel shaft (156 $\text{N}/\mu\text{m}$).

To measure the pitch stiffness, the same equipment was used as in the radial test except one contact was removed to apply a moment to the bearing. The flexure shown in Figure 1 was thinned in the center to allow rotation of the loading plate. For the moment experiments, a new stiffer flexure with no cutouts was fabricated. In this experiment two gage heads, one on each side of the bushing, were used. This orientation allowed the rotation of the shaft to be determined. The measured pitch stiffness was 5.5 $\text{N}\cdot\text{m}/\text{milli-radian}$ which is close to stiffness quoted by New Way of 5.3 $\text{N}\cdot\text{m}/\text{milli-radian}$ [2].

Dynamic Air Bearing Measurements

The two factors that were the focus of the bushings dynamics experiments were natural frequencies and noise. Natural frequencies were obtained by measuring one end of the shaft with a capacitance gage while tapping the other end of the shaft. The signal analyzer then output the natural frequencies of the shaft on the pressurized air film. The first natural frequency, a rigid body pitch mode, was observed at about 700 Hz. The results are shown in Figure 3. The top plot is the time series of the shaft motion resulting from a single tap showing a peak spacing of 1.43 msec or 700 Hz. The lower plot is the frequency spectrum of the top plot that shows peaks at 590 and 690 Hz.

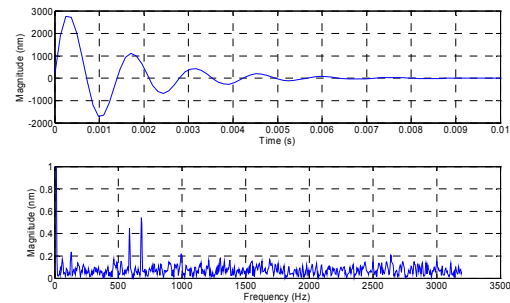


FIGURE 3. Radial motion of shaft when tapped in bushing measured by a capacitance gage.

The second reason for looking at the dynamics of the bushing was to determine the steady state vertical motion of the porous type bearing compared to the current FLORA. This experiment was the same as before except there was no excitation. A baseline recording of

the shaft sitting in the bearing is shown in Figure 4. Figure 4 shows that the bushing has a peak-to-peak motion of ± 4 nm. This is noise from the cap gage. Recall that FLORA had a motion of ± 100 nm which is significantly larger than the bushing. This finding reinforces the idea that porous air bearings are the right choice for use in FLORA I.

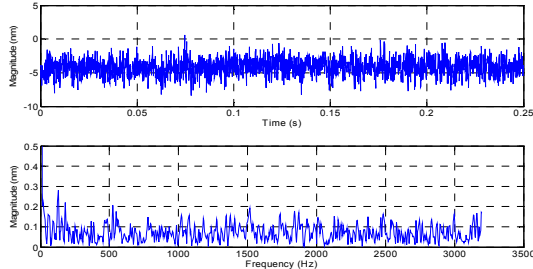


FIGURE 4. Steady-state vertical motion of shaft in bushing measured by a capacitance gage.

ANALYTICAL APPROACH

To compare the results of the experiments and ANSYS simulations of the bearing stiffness, equivalent radial and pitch stiffness are needed. The approach that was taken for both cases was to use a bed-of-springs approximation where the air bushing is modeled as a series of springs connected the shaft to the inside the bushing.

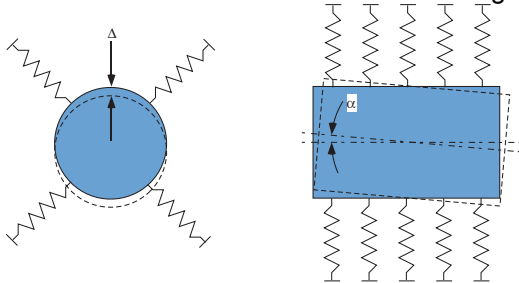


FIGURE 5. Bed of Springs approximation for radial stiffness (end view of shaft) and pitch stiffness (side view at right).

Equivalent Radial Stiffness

It is assumed that the equivalent radial stiffness will be a function of the radial stiffness provided by New Way. The equivalent stiffness was derived using an end view of the shaft as shown at left in Figure 5 to visualize the deflection of the springs. F_A is the applied force and Δ is the vertical translation of the shaft.

Using this model, the equivalent radial stiffness was derived as

$$k_A^r = \frac{2k_{NW}^r}{A_s} \quad (1)$$

The symbol k_A^r is the equivalent radial stiffness that is input into ANSYS and k_{NW}^r is the radial stiffness that is provided by New Way. The variable A_s is the surface area of the shaft inside the bushing. The equivalent radial stiffness is then used in a simulation of the shaft in FEA and the results is a stiffness of 34.1 N/um. FEA simulation with the derived stiffness behaves just like the physical bushing.

Equivalent Pitch Stiffness

As in the derivation of the equivalent radial stiffness, it was known that the equivalent pitch stiffness was going to be a function of the pitch stiffness that New Way provides. Figure 5 also shows a side view of the shaft that was used to derive a model of the equivalent pitch stiffness, which again must be done because the elastic foundation being used in ANSYS is stiffness per unit area. M is the applied moment and α is the pitch angle of the shaft. Using Figure 5, the following expression for the equivalent pitch stiffness is derived

$$k_A^p = \frac{24k_{NW}^p}{L^2 A_s} \quad (2)$$

k_A^p is the equivalent pitch stiffness for ANSYS and k_{NW}^p is the pitch stiffness provided by New Way. A_s is the surface area of the shaft inside the bushing and L is the length of the shaft. The equivalent pitch stiffness is simulated in FEA with a moment applied to the shaft. The rotation observed in the simulation replicates the behavior of the bushing.

A natural frequency simulation was also run in ANSYS using the equivalent stiffness which produced the bushing/shaft couplings first rigid body mode (pitch) at 700 Hz. This is the same value determined in the experiment shown in Figure 4.

PISTON CROSS SECTION

Three different piston cross sections were evaluated: box, triangle, and cross. ANSYS simulations were run to represent operating forces that the piston would encounter. Each cross section had equal length and mass to have as accurate a comparison as possible. After the simulations were run, each piston received a score based on performance to chose the superior cross section.

TABLE 1. Results from FEA simulations run on pistons with various cross sections

Scenario	Triangle	Box	Cross
End Load	3	1	2
Pressure	1	2	3
Bending	2	3	1
Rigid Body	2	2	1
Assembly	3	2	1
Total	11	10	8

A score of 3 was given to the cross section that performed the best while the worst received a 1. The end load test represented a vertical end load like the piston would see while machining. Pressure was the ability for a piston to withstand deformation from pressure applied by the bearings. Bending examined the first bending mode of the piston while rigid body was the first rigid body mode of the piston on the bed-of-springs approximation of the air bearing. Assembly refers to degree of difficulty in manufacturing each piston. The triangles ease of assembly is what made it more attractive than the box design.

PISTON MATERIAL

Choosing a material for the new piston will influence its mass and stiffness. Steel is a very stiff material but has a higher density, and potentially more mass, than competing materials for the application. A stiff, lightweight material is optimal. Aluminum was also considered which is 1/3 the density of steel but also 1/3 of the modulus. Aluminum is a good option, but to get a higher ratio of stiffness to density, composites were examined. After this study, one material that stood out was silicon carbide ceramic. Table 2 shows a comparison between steel, aluminum, and silicon carbide.

TABLE 2. Properties for piston material

Material	Modulus (Gpa)	Density (kg/m ³)	Modulus/Density (m ² /s ²)
Al	70	2700	26
Steel	200	7900	25
SiC	410	3150	130

It is clear that silicon carbide has a superior stiffness to mass ratio (5 times that of aluminum

and steel) and that is why this material has been chosen for the FLORA II piston.

CONCLUSIONS

The analytical derivation, experimental verification, and FEA simulation that was described earlier in this section all lead to the new FLORA II design shown in Figure 6. The housing dimensions in mm are 90H x 110W x 208L with motor. The piston is 70 mm in width across its top and 150 mm long with a moving mass of 250 g. Six porous air bearings provide stiffness for the piston which is driven by a voice coil motor. A linear encoder reads a glass scale attached to the piston for position feedback. As a comparison, the FLORA housing dimensions (mm) are 130H x 205W x 305L with motor and a moving mass of 650 g. The effort described in this section led into a new design for the FLORA II that will improve optical quality of NRS surfaces while reducing the size and mass of the actuator.

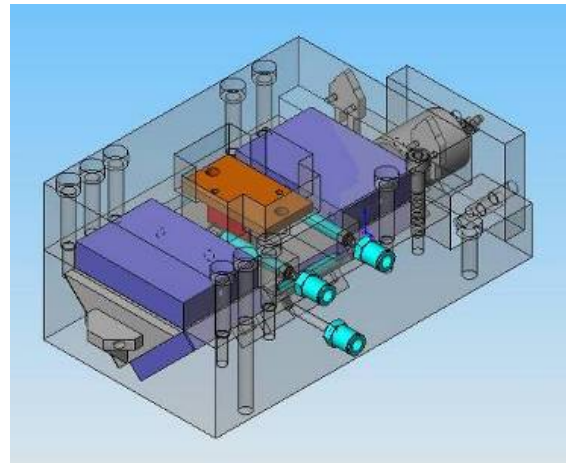


FIGURE 6. Isometric view of FLORA II with housing and base plate translucent.

ACKNOWLEDGEMENT

Principle funding for this research is through the NSF Grant DMI-0556209 monitored by G. Hazelrigg.

REFERENCES

- [1] Q. Chen, T. Dow, K. Garrard and A. Sohn, 2007. "A Fast Long Range Actuator", Proc. of ASPE, Vol 42, pg 287-290, 2007.
- [2] Newwayairbearings.com. Pennsylvania: New Way Air Bearings, Inc.;